NASA TN D-230

NASA TN D-230

7N-18
198496
43 P

TECHNICAL NOTE

D-230

THE VARIATION AND CONTROL OF RANGE TRAVELED IN THE ATMOSPHERE BY A HIGH-DRAG VARIABLE-LIFT ENTRY VEHICLE

By Donald C. Cheatham, John W. Young,
and John M. Eggleston

Langley Research Center
Langley Field, Va.

NATIONAL AERONAUTICS AND SPACE ADMINISTRATION

WASHINGTON March 1960

1J

NATIONAL AERONAUTICS AND SPACE ADMINISTRATION

TECHNICAL NOTE D-230

THE VARIATION AND CONTROL OF RANGE TRAVELED IN THE ATMOSPHERE BY A HIGH-DRAG VARIABLE-LIFT ENTRY VEHICLE

By Donald C. Cheatham, John W. Young,
and John M. Eggleston

L
8
3
0

SUMMARY

A study has been made of the variation of range traveled during the atmospheric entry phase of a high-drag variable-lift type of entry vehicle. The effect on range of such factors as entry angle, angle of attack, wing loading, initial velocity, orbital heading, and initial latitude was investigated. The data are presented in the form of charts showing the effect of each variable for entries starting at velocities close to circular satellite velocity. By using such a method, the range that will be traveled during the entry of a particular vehicle can be predicted for any combination of entry angle, wing loading, angle of attack, orbital heading, and initial latitude within the range covered by the analysis. Variations in range with variations in initial velocity can be accounted for during nonlifting entries. However, for lifting entries the variation in range with initial velocity is nonlinear and is difficult to predict.

Results are also presented which show the feasibility of an automatic control which regulates angle of attack in such a manner as to control the trajectory of the vehicle to a desired landing area. This method of range control involves the concept of controlling the vehicle's trajectory to a reference trajectory which terminates at the desired landing area. Results using this method of range control show that the range could be controlled to within ±20 miles of the desired location by the time an altitude of 100,000 feet is reached.

INTRODUCTION

In order to insure the recovery of an entry vehicle after it has reached the surface of the earth, it is necessary that the vehicle land in a predesignated area. The size of the area might be governed by the effectiveness of recovery facilities in the case where the final descent would be by parachute. In the case of an entry vehicle which has glide landing capabilities such as one conforming to the concept described in reference 1, the designated area may be reduced to the size of an ordinary landing field. In either case the ability to reach the designated area would be a function of how closely a desired entry trajectory outside the atmosphere can be reached and to what extent the trajectory within the atmosphere can be controlled.

A closed-form solution is not available for the distance (that is,
range) traveled by a point mass entering the earth's atmosphere on a
physically possible trajectory. Even solutions which assume small L
flight-path angles (ref. 2), constant deceleration (ref. 3), or constant 8
rate of descent (ref. 3) lead to solutions which require a point-by- 3
point (incremental) calculation of range as a function of at least one 0
other trajectory variable. Until a closed-form solution is found, it appears necessary to investigate the effects of each variable separately and to try to find some empirical method of predicting and controlling range based on any instantaneous value of each of the trajectory variables. Such an analysis is reported in this paper by considering one type of satellite vehicle returning to earth. The type of vehicle considered is one capable of high drag and low variable lift. Therefore, this analysis is applicable to any vehicle having a high-drag frontal surface and which is capable of generating a small lift-drag ratio up to about a lift-drag ratio of 0.5. For the purpose of visualizing the type of configuration, the drag surface is assumed to be essentially flat and nearly normal to the velocity, in which case the angle of attack is considered to be near 90° during the entry.

References 1 and 3 discuss the entry of a high-drag variable-lift class of entry vehicles and present results which show that small lift forces may be used to vary the distance traveled from the point of entering the fringe of the atmosphere (considered at 350,000 feet) to the landing area. The effectiveness of these lift forces in varying the range was very dependent upon just how the lift forces were programed. In order to develop procedures for programing lift forces that will result in accurate control of range, it is desirable to know the factors which influence range and the extent of this influence. The purpose of this paper is to determine the effects upon range caused by such factors as entry angle, angle of attack, velocity, wing loading, entry latitude, and orbital heading. In addition, results will be presented showing the feasibility of an automatic control which regulates angle of attack in order to control the entry trajectory of a high-drag, low-lift entry vehicle to a desired landing area.

SYMBOLS

L830

A	initial orbital heading angle, deg
a	acceleration, ft/sec^2
B	constant used in exponential approximation of atmospheric density
C_R	resultant-force coefficient
C_1,C_2	gain constants used in range controller (eq (8))
E_1,E_2,E_3	Euler angles used to orient two axes systems with respect to each other
a_F	acceleration due to aerodynamic force, $\frac{\text{Aerodynamic force}}{\text{Mass}}$, ft/sec^2
g	acceleration due to gravity, ft/sec^2
h	height above surface of earth, ft
H	angle between polar inertial X-axis and polar earth X-axis deg $\left(\dot{H} = \omega_E\right)$
$\vec{i},\vec{j},\vec{k}$	unit vectors along X-, Y-, and Z-axes, respectively
I_X,I_Y,I_Z	moments of inertia about principal body axis, slug-ft^2
K_1,K_2,K_3,K_4	constants used in expressions for range and maximum deceleration (eqs. (9) and (10))
l_1,l_2,l_3; m_1,m_2,m_3; n_1,n_2,n_3	direction cosines
L/D	lift-drag ratio
L	latitude, deg

L_c colatitude, deg

m mass of vehicle, slugs

$M_{Y,q}$ pitching moment due to pitching velocity, ft-lb

$M_{Y,\alpha}$ pitching moment due to angle of attack, ft-lb

$M_{Y,\delta}$ pitching moment due to elevator deflection, ft-lb

L
8
3
0

$M_{Z,r}$ yawing moment due to yawing velocity, ft-lb

$M_{Z,\beta}$ yawing moment due to angle of yaw, ft-lb

$M_{Z,\delta}$ yawing moment due to rudder deflection, ft-lb

p,q,r angular velocities about X-, Y-, and Z-axes, respectively, radians/sec

$\bar{q}$ dynamic pressure, lb/sq ft

R radial distance measured from earth's geographic center

S surface area, sq ft

Δs perimetric distance traveled over surface of earth since zero time (range), statute miles

t time, sec

u component of velocity along X-axis, ft/sec

v component of velocity along Y-axis, ft/sec

V velocity, ft/sec

w component of velocity along Z-axis, ft/sec

W weight of vehicle, lb

a_{Xb} acceleration due to aerodynamic force along X body axis, ft/sec^2

X,Y,Z orthogonal axes

α angle of attack, deg

β angle of sideslip, deg

γ flight-path angle, deg

δ_e elevator deflection, deg

δ_r rudder deflection, deg

ϵ_r range-to-go error, statute miles

L830

η inertial longitude, deg

λ longitude, deg

ψ,θ,ϕ Euler angles used to orient vehicle axes with respect to local earth axes

ρ atmospheric density, slugs/cu ft

ω_E angular velocity of earth

Ω angular velocity, radians/sec

Subscripts:

o value of variable at zero time

b body axes

z polar inertial axes

p polar earth axes

e earth stabilized axes

a wind axes

max maximum

X component along X-axis

Y component along Y-axis

Z component along Z-axis

T trim

A dot above a quantity denotes differentiation with respect to time. The symbol $\rightharpoondown$ above a quantity denotes a vector quantity.

METHODS AND ASSUMPTIONS

General

The effects upon the distance traveled during the atmospheric phase of a high-drag, low-lift entry vehicle caused by variations in such factors as angle of attack, wing loading, and so forth, have been determined by solving the equations of motion which describe the entry trajectory. The effect that a particular variable had on the range was determined by solving the equations of motion with different initial values of that variable. Much of the information was obtained with a fairly simple two-degree-of-freedom analysis of trajectories about a nonrotating earth. In order to determine effects associated with a rotating earth and atmosphere, a more sophisticated set of equations were used. For purposes of identification, these equations are termed nonrotating-earth equations and rotating-earth equations.

L
8
3
0

Nonrotating-Earth Equations

The force equations in this category are written to equate forces along and perpendicular to the vehicle's flight path. These equations, as derived in reference 3, are:

$$\dot{V} = \frac{-C_R \rho S \sin \alpha V^2}{2m} - g \sin \gamma \qquad (1)$$

$$\dot{\gamma} = \frac{C_R \rho S \cos \alpha V}{2m} + \frac{g}{V}\left(\frac{V^2}{gr} - 1\right)\cos \gamma \qquad (2)$$

$$\dot{h} = V \sin \gamma \qquad (3)$$

$$\Delta s = \int_0^t V \cos \gamma \, dt \qquad (4)$$

For the analysis made with these equations, it was assumed that in the high angle-of-attack conditions, the vehicle acted as a flat plate normal to the airstream and the resultant aerodynamic forces remained perpendicular to the face. A resultant-force coefficient $C_R = 1.7$

was assumed in accordance with preliminary information from wind-tunnel tests. The resolution of this resultant force into lift and drag forces shows a negative lift-curve slope. It should be noted that vehicles with lift coefficients other than the one assumed could obtain the same change in lift by making larger or smaller changes in angle of attack.

The earth was assumed to be spherical with a radius of 4,000 statute miles. A constant gravitational field of 32.2 ft/sec^2 was assumed throughout the altitudes covered. The earth was assumed to be stationary in all respects and there was no relative movement of the atmosphere.

Atmospheric density was assumed to vary according to the relation $\rho = \rho_o e^{-Bh}$ where $\rho_o = 0.003$ and $B = 1/23,000$. (These constants give a good approximation of the 1956 ARDC variation of atmospheric density in the region between 100,000 feet and 350,000 feet.)

Rotating-Earth Equations

The force equations solved in the analysis which account for the rotation of the earth's atmosphere as derived in the appendix are as follows

$$\ddot{L}_c = \frac{a_{Xe}}{R} - \frac{2\dot{h}\dot{L}_c}{R} + \dot{\eta}^2 \cos L_c \sin L_c \tag{5}$$

$$\ddot{\eta} = \frac{a_{Ye}}{R \sin L_c} - \frac{2\dot{h}\dot{\eta}}{R} - 2\dot{L}_c\dot{\eta}\frac{\cos L_c}{\sin L_c} \tag{6}$$

$$\ddot{h} = -a_{Ze} + R\dot{L}_c^2 + R\dot{\eta}^2 \sin^2 L_c \tag{7}$$

The distance traveled during an entry was assumed to be the great-circle-route distance between the initial-condition latitude and longitude and the final latitude and longitude.

As in the nonrotating-earth equations, the vehicle aerodynamics were assumed to be the same as a flat plate normal to the airstream. A resultant-force coefficient of 1.7 was assumed at an angle of attack of 90°; however, a further assumption that this coefficient varied approximately as the sine of the angle of attack was included.

The earth, for the analysis made with these equations, was assumed to be spherical with a radius of 3,963 statute miles. The gravitational field was assumed to be constant at 31.2 ft/sec^2. (This is the calculated gravity force at an intermediate altitude of 200,000 ft.)

The atmosphere was assumed to rotate with the earth and no relative movement (wind shear) was assumed. The atmospheric density was assumed to vary in accordance with the 1956 ARDC model (ref. 4).

Automatic Range Control Equations

L830

The method of range control studied is based upon the concept of controlling the entry to a reference trajectory which terminates at the desired destination. The reference trajectory is a calculated trajectory based on the best available data (atmospheric density, drag coefficient of the vehicle, and so forth) for the vehicle considered. The point at which the trajectory terminates is designated as zero. Thus every other point on the trajectory has a corresponding "range-to-go" to this terminal point.

Two types of reference trajectories were used in controlling range. The first, designated as type I, is shown in figure 1(a). Such trajectories are obtained by holding a constant angle of attack throughout the entry and by initiating the entry with three different flight-path angles at an altitude of 350,000 feet. For simplicity the actual $h - \Delta s$ curves were assumed to be straight lines above an altitude of 230,000 feet* and to follow the same trajectory below 230,000 feet. Based on these assumptions the data of figure 1(a) were fitted with a simple equation of range-to-go as a function of altitude and initial entry angle. The second type of reference trajectory, known as type II, is shown in figure 1(b). The type II trajectory is obtained by joining the actual entry point and the 230,000-foot point by a straight line as shown in figure 1(b). For comparison, a type I reference trajectory is also shown in figure 1(b). It should be noted that the type I reference trajectory is defined by the initial entry angle whereas the type II reference trajectory is defined by the desired range. During the entry of a vehicle it is presumed that equipment will be available to measure accurately the altitude and the distance between the position of the vehicle and the desired destination. By comparing this information with data of the reference trajectory, an error in range-to-go can be determined. It was assumed that the differential of range-to-go error could also be obtained. The rate of change of the range-to-go error would probably be obtained by a process of differentiation of the range-to-go error signal in any practical system. Because differentiation normally results in undesired noise on the signal, fairly heavy filtering would probably be used. However, because changes in the entry trajectory

---

*This altitude would vary with wing loading and trim angle of attack.

are of a rather low frequency, the filter dynamics would have a relatively insignificant effect on the trajectory dynamics. Therefore, no noise or filtering was included in the present analysis.

These quantities, range-to-go error, and rate of change of range-to-go error, are modified by gain constants and combined to command a desired angle of attack for purposes of automatic range control. The angle of attack commanded is such that, if the vehicle is short of the reference trajectory, a lower angle is commanded in order to obtain positive lift that will tend to lengthen the trajectory. The equation utilized for this command is as follows:

$$\alpha = \alpha_T - C_1\epsilon_r + C_2\dot{\epsilon}_r \tag{8}$$

where α_T is the trim angle associated with the reference trajectory and C_1 and C_2 are gain constants. The error in range-to-go is determined by

$$\epsilon_r = (\text{Range-to-go}) - (\text{Reference range-to-go}) \tag{9}$$

SCOPE OF TESTS

Factors Influencing Range

It is realized that, for any particular vehicle, very detailed calculations of trajectories will be carried out. The data presented here are not sufficient to replace such calculations but are intended to show trends. Therefore, the entire spectrum of possible combinations of initial altitude, velocity, flight-path angle, and so forth is not considered but a representative cross section is studied. By holding constant all but one of the important parameters and then methodically changing that one parameter during successive computed entries, the effect of the parameter on the distance traveled by the vehicle can be studied.

Most of the data were obtained for entries with a vehicle having a wing loading of 20 pounds per square foot and traveling at circular satellite velocity at the initial point of reentry. With these conditions, runs were made over an entry-angle range from 0° to -5° and wit the angle of attack varied from 100° to 60°.

The effects on the range of changes in wing loading were investigated by using the nonrotating-earth analysis. Tests were made with wing loadings of 10, 40, and 60 pounds per square foot over the entry-angle range from -1° to -5° for a constant angle of attack of 90°. In addition, limited calculations were made at an entry angle of -1° to determine the influence of wing loading upon the variation of range with angle of attack.

The effects of entering at velocities other than equilibrium or circular satellite velocity were determined over the range of velocities from 24,000 to 28,000 feet per second for nonlifting reentries beginning at entry angles of -1° to -5°. These calculations were made by using the nonrotating-earth equations.

L 8 3 0

The rotating-earth equations were utilized to investigate the effect of initial heading and latitude at entry upon range traveled with respect to the earth. Entry angles from 0° to -5° were covered. The tests covered a complete 360° range of headings for entries at the equator and at a latitude of 45°. Limited calculations were also made to determine how the influence of angle of attack differs with entry heading.

Automatic Range Control

The tests of the automatic-range-control concept were made at entry angles of -1°, -2°, and -3° and all started at an equilibrium velocity of 25,863 feet per second. The reference trajectories used in these tests are shown in figures 1(a) and 1(b). The initial range-to-go error was varied from -200 miles to 900 miles for the -1° entries, from -100 miles to 400 miles for the -2° entries, and from -150 miles to 250 miles for the -3° entries.

The gains used in equation (8) to compute desired angle of attack were established by trial-and-error methods. In some cases the gain on the range-to-go error signal was varied in a linear fashion with altitude. In all cases limits of 60° and 110° were imposed on the angle of attack.

RESULTS AND DISCUSSION

Nonrotating Earth

Effect of flight-path angle and angle of attack upon range.- The effect of angle of attack upon the range traveled during the entry of a high-drag, variable-lift vehicle is illustrated in the plots shown in figure 2. The profile of altitude plotted against range shows a typical variation that results when small lift forces are generated by an angle of attack less than 90° (in this case, 79°). For comparison a nonlifting ($\alpha = 90^\circ$) case is also shown. The principal effects upon the trajectory with regard to range traveled occur at altitudes between 300,000 feet and 175,000 feet. For steeper entry angles, a slightly lower altitude is reached before the effects of positive lift became apparent in the range and deceleration. The profile of deceleration shows the marked effect of angle of attack that has been previously described in references 1 and 3.

A summary plot of the range traveled by a high-drag vehicle at a constant L/D is shown in figure 3. For convenience, the ordinate is given in both L/D and angle of attack since the latter is used in all succeeding figures. The abscissa gives the distance traveled from the initial altitude of 350,000 feet, the initial velocity of 25,863 feet per second, and the indicated initial flight-path angles. It can be seen that the variation of range with angle of attack for a given entry angle is nonlinear and is shown to be relatively insensitive to changes in angle of attack at angles of attack of 90° and above but increases in sensitivity at lower angles of attack.

L-830

Effect of initial velocity upon range.- The data presented previously in figures 2 and 3 apply to entries which start with a velocity of 25,863 feet per second at 350,000 feet and with a wing loading of 20 pounds per square foot. However, the velocity used to calculate the data presented in figures 2 and 3 may not be the velocity at which an actual entry will occur. Therefore, it is of interest to determine the relative effect of initial velocity with range. Figure 4 shows the effect of various values of initial velocity upon the range traveled during nonlifting entries ($\alpha = 90^{\circ}$) for entry angles from -1° to -5°. At -5° the range traveled is approximately a linear function of velocity with a slope of only 0.0175 mile per foot per second over the range of velocities from 24,000 to 28,000 feet per second. As the entry angle is decreased below -3°, the variation of range with velocity becomes nonlinear and, in the case of the -1° entry, the sensitivity varies from about 0.2 mile per foot per second at an initial velocity of 24,000 to a sensitivity of almost infinity at a velocity of 26,500. This latter velocity is the condition in which the vehicle will not be captured by the atmosphere but the trajectory will continue back outside the atmosphere for most of another orbit.

In order to determine the effect of velocity on lifting entries, a number of entries were made with four different initial velocities (24,000 to 26,000 feet per second) and with constant angles of attack (60° to 90°). The entry angle in all cases was -1°. The results are shown in figure 5. It can be seen from figure 5 that the distance traveled is not only a nonlinear function of the initial velocity but is also a nonlinear function of the angle of attack during the entry. Limited calculations at entry angles of -2° and -3° indicate that the nonlinearities are less pronounced for these larger entry angles.

<u>Effect of wing loading upon range</u>.- The variations of range traveled for nonlifting entries over the entry-angle range from -1° to -5° for wing loading of 10, 20, 40, and 60 pounds per square foot are shown in figure 6. An initial velocity of 25,863 feet per second and an initial altitude of 350,000 feet were used for all entries. The data of figure 6 show that, as the wing loading is increased, the range is also increased. The reason for the increase in range is that vehicles having a higher wing loading also have greater kinetic energy per unit area.

The variation of range traveled for lifting entries for different
wing loadings is shown in figure 7 for cases where the entry angle L
was -1°. The figure shows that the variation in range with angle of 8
attack is virtually independent of the wing loading and that the increase 3
in range with increased wing loading may be accounted for with the addi- 0
tion of a constant which is proportional to $\log_e (W/C_R S)_1 / (W/C_R S)_2$.

Rotating Earth and Atmosphere

<u>Effect of angle of attack and flight-path angle upon range</u>.- The variation of range with flight-path angle and angle of attack for cases where the earth and atmosphere are assumed to rotate at the normal sidereal rate are shown in figure 8. Variations are presented for cases where the orbital heading is to the south (180°) and to the east (90°). For both cases the entry was initiated at the equator. It can be seen that there is a significant effect of heading angle upon range and that this effect is most prominent at the smaller entry angles and the lower angles of attack. As expected the entries made with headings of 180° resulted in values of range in good agreement with the data of figure 3 for a nonrotating earth. The indication is then that the slight differences in density variation (ARDC variation compared with exponential variation) and variation of resultant-force coefficient (constant times the sine α compared with a constant) had negligible effects upon the calculated variation of range traveled for given conditions of initial flight-path angle and angle of attack.

<u>Effect of heading and latitude at entry upon range</u>.- In order to determine the effect of heading angle and latitude on range, trajectories were calculated for entries with heading angles from 0° to 360° for latitudes of 0° and 45°. Figure 9 shows the result of these runs for an entry angle of -1° and an angle of attack of 90°. The data are plotted to show the relationship of range traveled and peak deceleration encountered as a function of heading angle. The calculated data points are indicated by the symbols and the pattern that was formed had the appearance of a sine wave. Hence, an attempt was made to derive a relationship which would closely approximate the calculated data. A simple relationship that was found to satisfy this requirement was of the form

$$\text{Range} = K_1 - K_2 \sin A \cos L \tag{9}$$

(The term $\sin A \cos L$ is equivalent to the cosine of the orbit inclination angle.) The curves shown in figure 9 were calculated from this expression where $K_1 = 1,345$ and $K_2 = 58$. The variation of peak deceleration followed a similar relationship with heading and latitude and the peak g was approximated by the relationship

$$g_{max} = K_3 - K_4 \sin A \cos L \tag{10}$$

where $K_3 = 6.95g$ and $K_4 = 0.6g$.

L-830

The significance of the range variation with heading as illustrated on figure 9 is that the rotation of the earth beneath the vehicle as it enters has a larger effect upon range than that which is attributed to the difference in drag due to the change in airspeed with heading. In other words, the decrease in g that is obtained by entering to the east gives only a small increase in range relative to the surface of the earth compared with the decrease in range due to the rotation of the earth during the time required for the entry.

The sinusoidal variation of range with initial heading shown in figure 9 for the case of an entry angle of -1° was also found at all entry angles from -1° to -5°. The variation of range traveled and the peak deceleration encountered could be well approximated by expressions (9) and (10) but with different values of the parameters K_1, K_2, K_3, and K_4. The variations of K_1 and K_2 over the entry-angle range from -1° to -5° are shown in figures 10(a) and 10(b) for a wing loading of 20 pounds per square foot and an angle of attack between 100° and 70°. The variation of K_1 with flight-path angle and angle of attack shows the range variation which would be expected for nonrotating-earth analysis. The magnitude of K_2, for an angle of attack of 90°, varies from about 90 miles at an entry angle of 0° to about 22 miles at $\gamma = -5^\circ$. The time required from the point of entry to the point where the peak g is reached varies in almost the same manner with flight-path angle as does the magnitude of K_2.

The variations of K_3 and K_4 over the entry-angle range from 0° to -5° are shown in figure 11 for a wing loading of 20 pounds per square foot and an angle of attack of 90°. The magnitude of K_4 is relatively constant over the range of γ from 0° to -5° and varies only from 0.6 to about 0.9. Therefore, the maximum deceleration obtained during an entry is only slightly dependent upon the latitude and heading angle and cannot vary more than 1 g because of these factors. The maximum deceleration is influenced predominantly by the entry angle and it is noted that K_3 has a variation with entry angle similar to that calculated by Chapman in reference 2. (See fig. 20(a).)

Effect of wing loading upon range.- The effect of wing loading upon the range traveled and the peak deceleration encountered is shown in figure 12 for -1° entries. Variations are shown for both southerly and easterly orbital headings at entry. (Entry is at 0° latitude.) The variation of the cases starting with southerly headings is essentially the same as that presented in figure 6 for the nonrotating-earth analysis. The variation representing the easterly heading shows an approximately constant 65-mile shift in range and 0.6g shift in peak deceleration throughout the wing-loading range. Because the difference in range traveled between entries starting with easterly headings and those starting with southerly headings is essentially equivalent to the value of K_2 in the range expression of equation (9), the data of figure 12 indicate that variations in wing loading primarily affect the magnitude of K_1 and have a negligible effect upon K_2. Although this has only been confirmed for -1° entries, the steeper entries are basically less affected by wing loading and it is expected that the same trend of constant K_2 and increasing K_1 with increasing wing loading will hold true.

The discussion of the effect of wing loading throughout this report is based upon the assumption that the resultant-force coefficient has the value of 1.7. In the event that experimental data indicate that a different drag coefficient is applicable, the data associated with the various wing loadings may be converted to the appropriate value of the parameter $W/C_R A$ (such as was done in ref. 1) and would not lose its validity.

Range prediction.- In the preceding sections the relationship of range to such factors as entry angle, wing loading, angle of attack, initial velocity, orbital heading, etc., was established to a limited extent. For entries that start with initial velocities approximately equal to circular satellite velocity, the data presented are sufficient to predict the range traveled by a vehicle entering at any flight-path angle between -1° and -5°, with any wing loading between 20 and 60 pounds per square foot, at any angle of attack between 60° and 100°, and with any orbital heading and latitude at the entry point. As an illustration, consider the following example:

Consider the case of a vehicle having a wing loading of 40 pounds per square foot entering at -2° with an angle of attack of 80° on a heading of 045° at a latitude of 30°. From equation (9) the range is found to be $K_1 - K_2 \sin A \cos L$. From figure 10(a), K_1 for $\gamma = -2^{\circ}$,

$\alpha = 80^\circ$, $W/S = 20$ and a nonrotating earth is found to be 1,220 miles. Reference to figure 6 to correct for wing loading shows the correction to be 100 miles. The earth's rotation does not affect K_1 so its corrected value is $1,220 + 100 = 1,320$. From figure 10(b) the value of K_2 is found to be approximately 65 miles. Because wing loading does not affect K_2, no further corrections are necessary. Thus, the range traveled is $1,320 - 65 \sin 45^\circ \cos 30^\circ$ or 1,280 miles.

L830

The data utilized in this example could also be interpreted so as to determine an angle of attack required in order to obtain a specified range under given conditions of entry angle, wing loading, and so forth. This approach would, however, provide an open-loop type of range control that would be sensitive to errors in determining such quantities as flight-path angle, altitude, range-to-go, and so forth. Such a type of range control would require a rather complex computational procedure to take into account the factors affecting range such as was done in the example. Additional complexities would arise if variations in initial velocity would have to be accounted for.

Automatic Range Control

General.- A more simplified approach to range control than the open-loop predictor approach discussed in the previous section is afforded by the concept of controlling the entry to a reference trajectory. This approach is described in the section on methods and assumptions.

The operation of the range controller is illustrated in figures 13 and 14 where an entry starting with a flight-path angle of -1° is shown. The angle-of-attack controller follows the expression

$$\alpha = \alpha_T - C_1\epsilon_r + C_2\dot{\epsilon}_r$$

The variation of range-to-go with altitude shown in figure 14 presents an overall picture of how the trajectory is controlled to the reference. Figure 13 shows that the initial range error calls for an angle of attack close to 60°. As the range-to-go error decreases, the angle of attack increases toward 90° and, because of the effect of the rate of change of the range-to-go term, the angle of attack goes above the reference trim angle of 84° before the range-to-go error is zero. There is about a 50-mile overshoot in range-to-go error; however, this error is satisfactorily corrected and the error at the 100,000-foot altitude is less than 10 miles.

Accuracy of range-controller operation.- After preliminary checks were made to determine the appropriate value of the gains on the range-to-go error and range-to-go error rate, a number of runs were made to determine the accuracy with which the range controller could control the trajectory to a desired destination. The reference trajectory in each case was the one of the three shown in figure 1(a) which had the same initial flight-path angle as the test run. A plot of range desired and range obtained for runs starting with flight-path angles of -1°, -2°, and -3° are shown in figure 15. The solid symbols indicate the range of the reference trajectory for each entry angle. Most of the runs were made with gains of 0.06° per mile and 2° per mile per second. These gains gave accuracy within 10 miles for cases where the initial range- L
to-go to destination was greater than the reference trajectory. When 8
the initial range-to-go was 100 to 200 miles less than the reference 3
trajectory, range overshoots resulted that varied from about 25 miles 0
for a -1° entry angle up to 75 miles for a -3° entry angle. A few runs were made where the range-to-go error gain was increased to 0.1° per mile and these data are indicated by the flagged symbols shown in figure 15. The accuracy obtained with these gains was better for the shorter desired range cases than was obtained with the gain of 0.06° per mile and indicated that gain optimization could probably improve the range control accuracy somewhat. The intent of this study, however, was only to show the feasibility of such a method of range control and no further attempt was made to optimize the method.

A limited number of runs were made with a type II reference trajectory as shown in figure 1(b). The range-to-go error gain was increased to 0.14° per mile for these runs (C_2 held constant at 2°/mile/sec) and the results were essentially the same as those obtained with the tests with the upper segment of the reference fixed by the entry angle (type I) rather than by the entry point.

All the entry trajectories controlled by the range controller were calculated with the nonrotating-earth equations. However, there is nothing to indicate that such a controller would not work with the rotating-earth equations.

CONCLUDING REMARKS

The present study has shown that, if the velocity of a high-drag variable-lift entry vehicle is known at the point of entry, the influence on the range of such factors as entry angle, angle of attack, wing loading, orbital heading, and initial latitude can be predicted. Although velocity at entry may be known reasonably close in advance, range prediction by the use of such charts and equations as have been discussed in the previous sections is both complex and subject to errors due to measurement inaccuracies.

The concept of range control by controlling the entry to a reference trajectory which terminates at a desired destination has been shown to be feasible. The accuracy of this method of range control was reasonably good under the ideal conditions assumed in the present analysis. It is recommended, however, that further studies of such a method of range control be made in which factors such as the accuracy of measuring position, range-to-go, altitude, and so forth, be taken into account as well as possible deviations of atmospheric density and drag coefficients from that currently established. Further studies should also include methods for controlling the lateral range of an entry vehicle. An investigation of the navigational problem of entry vehicles of classes other than the high-drag variable-lift type is also recommended.

Langley Research Center,
National Aeronautics and Space Administration,
Langley Field, Va., November 23, 1959.

APPENDIX

EQUATIONS OF MOTION FOR ROTATING EARTH AND ATMOSPHERE

The following frames of reference are used in defining the motion of an entry vehicle entering the atmosphere of a rotating earth. The geometry is shown in figure 16. All axes systems are considered to be positive orthogonal.

L
8
3
0

$(X,Y,Z)_z$ polar inertial axes (fixed in space); the Z-axis is positive toward the North

$(X,Y,Z)_e$ earth-stabilized axes (origin at center of gravity of body); the Z-axis is positive toward the earth's center and the X-axis is positive toward the South

$(X,Y,Z)_p$ polar earth axes (fixed in earth); the Z-axis is positive toward the North

$(X,Y,Z)_b$ body axes (principal axes fixed in body)

$(X,Y,Z)_a$ wind axes (origin at center of gravity of body)

In order to orient these frames of reference with respect to each other, a general Euler angle transformation is defined. The three angles used to orient a moving frame of reference with respect to a reference frame are:

E_1 rotation about Z-axis

E_2 rotation about new position of Y-axis

E_3 rotation about final X-axis

Hence,

$$\begin{Bmatrix} X \\ Y \\ Z \end{Bmatrix}_{\text{Reference}} = \begin{bmatrix} l_1 & m_1 & n_1 \\ l_2 & m_2 & n_2 \\ l_3 & m_3 & n_3 \end{bmatrix} \begin{Bmatrix} X \\ Y \\ Z \end{Bmatrix}_{\text{Moving}}$$

where

$$\left.\begin{aligned}
l_1 &= \cos E_1 \cos E_2 \\
l_2 &= \sin E_1 \cos E_2 \\
l_3 &= -\sin E_2 \\
m_1 &= \cos E_1 \sin E_2 \sin E_3 - \sin E_1 \cos E_3 \\
m_2 &= \sin E_1 \sin E_2 \sin E_3 + \cos E_1 \cos E_3 \\
m_3 &= \cos E_2 \sin E_3 \\
n_1 &= \cos E_1 \sin E_2 \cos E_3 + \sin E_1 \sin E_3 \\
n_2 &= \sin E_1 \sin E_2 \cos E_3 - \cos E_1 \sin E_3 \\
n_3 &= \cos E_2 \cos E_3
\end{aligned}\right\} \tag{A1}$$

L
8
3
0

The rate of change of these Euler angles can be expressed by

$$\left.\begin{aligned}
\dot{E}_1 &= \frac{r \cos E_3}{\cos E_2} + q \frac{\sin E_3}{\cos E_2} \\
\dot{E}_2 &= q \cos E_3 - r \sin E_3 \\
\dot{E}_3 &= p + q \tan E_2 \sin E_3 + r \tan E_2 \cos E_3
\end{aligned}\right\} \tag{A2}$$

where p, q, and r are the components in the moving axes of the angular velocity along X, Y, and Z.

By using equations (A1) and (A2) it is seen that the rate of change of the direction cosines can be expressed by

$$\left.\begin{aligned}
\dot{l}_j &= m_j r - n_j q \\
\dot{m}_j &= n_j p - l_j r \\
\dot{n}_j &= l_j q - m_j p
\end{aligned}\right\} \qquad (j = 1,\ 2,\ \text{and } 3) \tag{A3}$$

The following symbolism is used

$$(X,Y,Z)_{reference} = \left[E_1,\ E_2,\ E_3\right](X,Y,Z)_{moving}$$

Hence from figure 16,

$$(X,Y,Z)_p = \left[\lambda,\ L_c,\ \pi\right](X,Y,Z)_e$$

$$(X,Y,Z)_z = \left[H,\ 0,\ 0\right](X,Y,Z)_p$$

$$(X,Y,Z)_z = \left[\eta,\ L_c,\ \pi\right](X,Y,Z)_e$$

$$(X,Y,Z)_e = \left[\psi,\ \theta,\ \phi\right](X,Y,Z)_b$$

$$(X,Y,Z)_e = \left[A,\ \gamma,\ 0\right](X,Y,Z)_{V_a}$$

where

η	inertial longitude, $\lambda + H$
L_c	colatitude
ψ,θ,ϕ	orientation of body axes with respect to local earth axes
A,γ	azimuth and elevation of velocity vector

The equations of motion are developed in the earth-stabilized axis system by applying the following general vector equations

$$\frac{d}{dt}\left(\vec{V}\right) = \vec{F} + \vec{g} = \frac{\overrightarrow{dV}}{dt} + \vec{\Omega} \times \vec{V} \tag{A4}$$

where Ω is the angular velocity of the axis system with respect to a specified reference system.

The velocity of the vehicle in the earth-stabilized axis system is given by

$$\begin{aligned}\vec{V} &= u\vec{i} + v\vec{j} + w\vec{k} \\ &= \dot{L}_c R\vec{i} - R\dot{\eta}\sin L_c\vec{j} - \dot{R}\vec{k}\end{aligned} \tag{A5}$$

The angular rotational rate of the earth-stabilized axis system with respect to the polar inertial axis system is given by

$$\Omega_{Ze} = -\dot{\eta} \sin L_c\vec{i} - \dot{L}_c\vec{j} - \dot{\eta} \cos L_c\vec{k} \tag{A6}$$

The force equations in the earth-stabilized axis system are found by substituting equations (A6) and (A5) and the derivative of equation (A5) into equation (A4). This procedure gives

L
8
3
0

$$\vec{F} + \vec{g} = \left(R\ddot{L}_c + 2\dot{R}\dot{L}_c - R\dot{\eta}^2 \sin L_c \cos L_c\right)\vec{i} + \left(-R\ddot{\eta} \sin L_c - 2\dot{R}\dot{\eta} \sin L_c - 2R\dot{L}_c\dot{\eta} \cos L_c\right)\vec{j} + \left(-\ddot{R} + R\dot{\eta}^2 \sin^2 L_c + R\dot{L}_c^{\,2}\right)\vec{k}$$

These equations can be expressed in the following form:

$$\left.\begin{aligned}
F_{Xe} + g_{Xe} &= R\ddot{L}_c + 2\dot{R}\dot{L}_c - R\dot{\eta}^2 \sin L_c \cos L_c \\
F_{Ye} + g_{Ye} &= -R\ddot{\eta} \sin L_c - 2\dot{R}\dot{\eta} \sin L_c - 2R\dot{L}_c\dot{\eta} \cos L_c \\
F_{Ze} + g_{Ze} &= -\ddot{R} + R\dot{\eta}^2 \sin^2 L_c + R\dot{L}_c^{\,2}
\end{aligned}\right\} \tag{A7}$$

By assuming a spherical earth with no oblateness effect, the components of g at an intermediate altitude of 200,000 feet are:

$$g_{Xe} = g_{Ye} = 0$$

$$g_{Ze} = g = 31.2 \text{ ft/sec}^2$$

Hence, equation (A7) can be expressed in the following manner:

$$\left.\begin{aligned}
\ddot{L}_c &= \frac{a_{Xe}}{R} - \frac{2\dot{h}\dot{L}_c}{R} + \dot{\eta}^2 \cos L_c \sin L_c \\
\ddot{\eta} &= \frac{a_{Ye}}{R \sin L_c} - \frac{2\dot{h}\dot{\eta}}{R} - 2\dot{L}_c\dot{\eta}\,\frac{\cos L_c}{\sin L_c} \\
\ddot{h} &= -a_{Ze} + R\dot{L}_c^{\,2} + R\dot{\eta}^2 \sin^2 L_c
\end{aligned}\right\} \tag{A8}$$

where $\dot{L} = -\dot{R}$ and where a_{Xe}, a_{Ye}, and a_{Ze} are the components of the acceleration in the earth-stabilized axis system and are given by

$$a_{Xe} = l_1 a_{Xb} = F_{Xe}$$

$$a_{Ye} = l_2 a_{Xb} = F_{Ye}$$

$$a_{Ze} = g + l_3 a_{Xb} = g + F_{Ze}$$

where

$$\left.\begin{aligned} a_{Xb} &= -\frac{C_R S}{m}\bar{q}\frac{u_b}{V} \\ \bar{q} &= \frac{1}{2}\rho V^2 \end{aligned}\right\} \tag{A9}$$

By definition,

$$\alpha = 90 + \tan^{-1}\frac{w_b}{u_b}$$

$$\beta = \sin^{-1}\frac{-v_b}{V}$$

where u_b, v_b, and w_b are defined by

$$\left.\begin{aligned} u_b &= l_1 u_e + l_2 v_e + l_3 w_e \\ v_b &= m_1 u_e + m_2 v_e + m_3 w_e \\ w_b &= n_1 u_e + n_2 v_e + n_3 w_e \end{aligned}\right\} \tag{A10}$$

From equation (A5)

$$\left.\begin{aligned} u_e &= R\dot{L}_c \\ v_e &= R\dot{\lambda} \sin L_c \\ w_e &= -\dot{h} = \dot{R} \\ V_e &= \left(u_e{}^2 + v_e{}^2 + w_e{}^2\right)^{1/2} \end{aligned}\right\} \tag{A11}$$

L
8
3
0

From figure 16

$$\left.\begin{aligned} A &= \tan^{-1}\frac{v_e}{u_e} \\ \gamma &= \sin^{-1} - \frac{w_e}{V} \\ \dot{\lambda} &= \dot{\eta} - \omega_E \end{aligned}\right\} \qquad \text{(A12)}$$

L
8
3
0

With the assumption that the body axes are the principal body axes and that Ω_{Ze} is negligible, the moment equations become

$$I_X\dot{p} = \left(I_Y - I_Z\right)qr + \text{Rolling moment}$$

$$I_Y\dot{q} = \left(I_Z - I_X\right)rp + \text{Pitching moment}$$

$$I_Z\dot{r} = \left(I_X - I_Y\right)pq + \text{Yawing moment}$$

The rolling velocity p was assumed to be zero; hence

$$\left.\begin{aligned} \dot{p} &= 0 \\ \dot{q} &= \frac{\text{Pitching moment}}{I_Y} = \frac{M_{Y,q}q}{I_Y} + \frac{M_{Y,\alpha}\alpha}{I_Y} + \frac{M_{Y,\delta}\delta_e}{I_Y} \\ \dot{r} &= \frac{\text{Yawing moment}}{I_Z} = \frac{M_{Z,r}r}{I_Z} + \frac{M_{Z,\beta}\Delta\beta}{I_Z} + \frac{M_{Z,\delta}\delta_r}{I_Z} \end{aligned}\right\} \qquad \text{(A13)}$$

The damping moment terms $\frac{M_{Y,q}}{I_Y}$ and $\frac{M_{Z,r}r}{I_Z}$ were made sufficiently large to damp out any small changes in α and β.

In order to obtain a given angle of attack, a computed constant control deflection was applied which, based on the static stability of the vehicle, would give a trim angle of attack equal to that desired.

REFERENCES

1. Staff of Langley Flight Research Division (Compiled by Donald C. Cheatham): A Concept of a Manned Satellite Reentry Which is Completed With a Glide Landing. NASA TM X-226, 1959.

2. Chapman, Dean R.: An Approximate Analytical Method for Studying Entry Into Planetary Atmospheres. NACA TN 4276, 1958.

3. Eggleston, John M., and Young, John W.: Trajectory Control for Vehicles Entering the Earth's Atmosphere at Small Flight-Path Angles. NASA MEMO 1-19-59L, 1959.

4. Minzner, R. A., and Ripley, W. S.: The ARDC Model Atmosphere, 1956. Air Force Surveys in Geophysics, No. 86 (AFCRC TN-56-204), Geophysics Res. Div., AF Cambridge Res. Center (Bedford, Mass.), Dec. 1956. (Available as ASTIA Doc. 110233.)

L
8
3
0

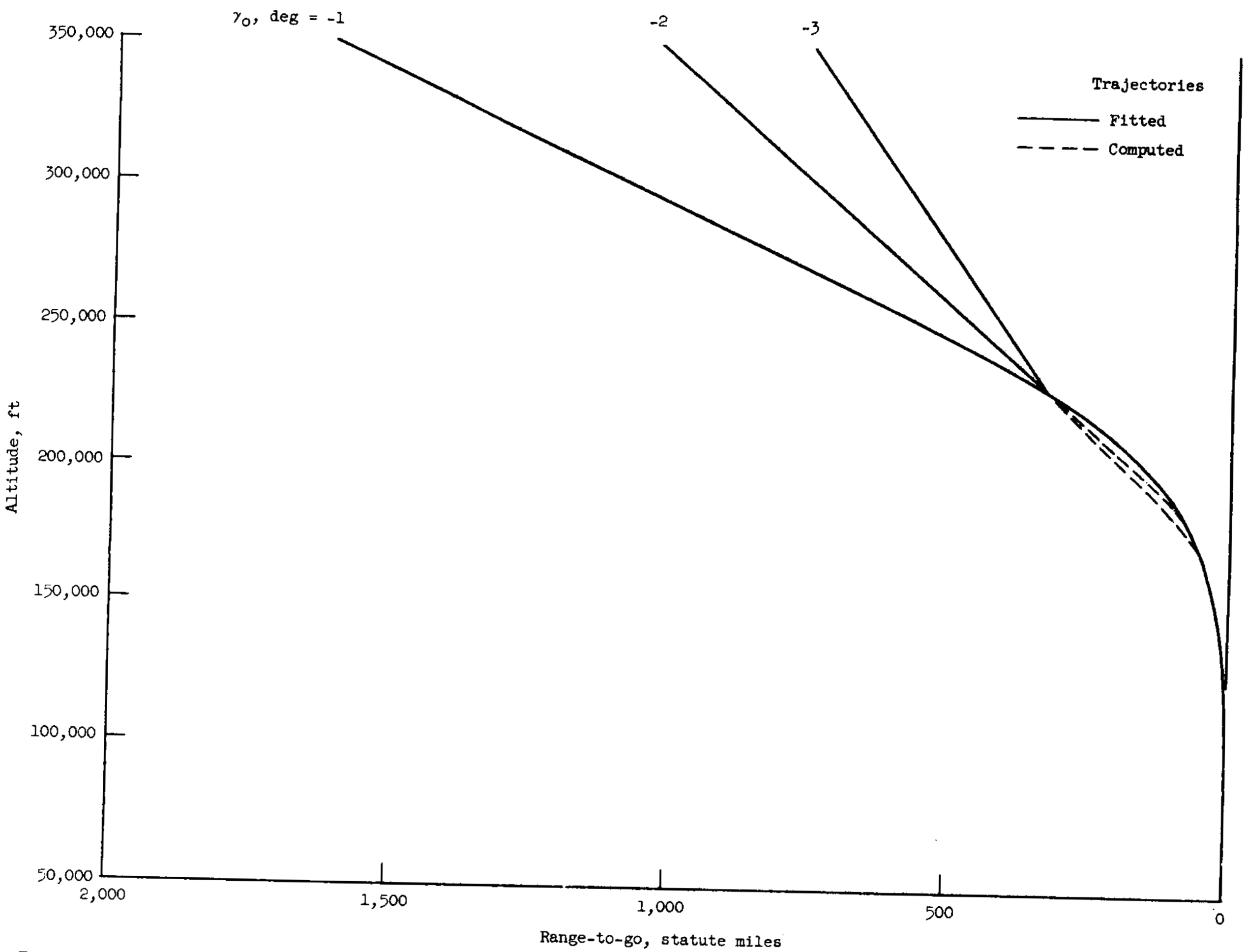

(a) Type I reference trajectory. $\alpha = 84^\circ$.

Figure 1.- Reference trajectories of range-to-go as a function of altitude.

$V_o = 25,863$ feet per second; $W/S = 20$ pounds per square foot.

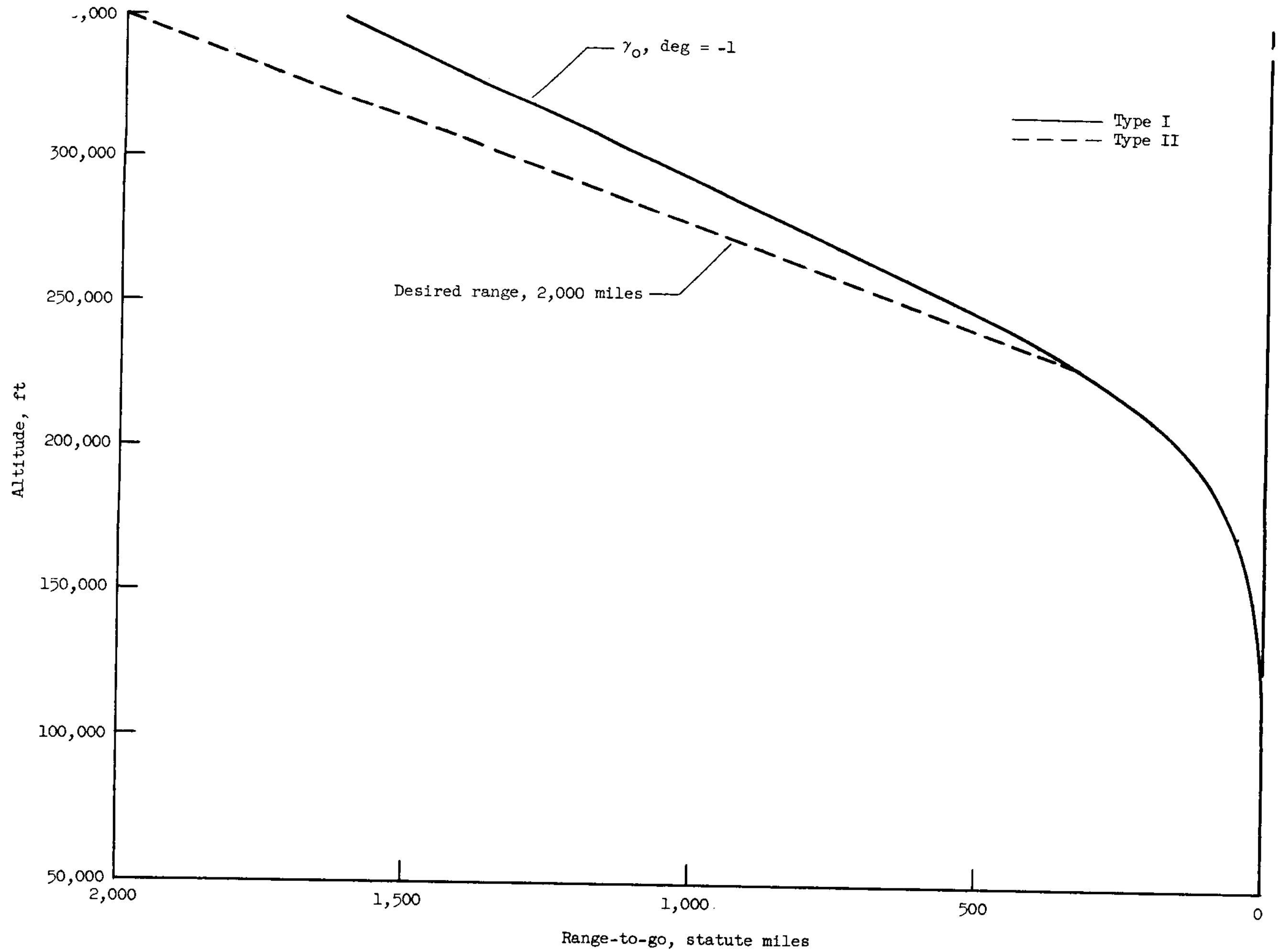

(b) Type I and Type II reference trajectories.

Figure 1.- Concluded.

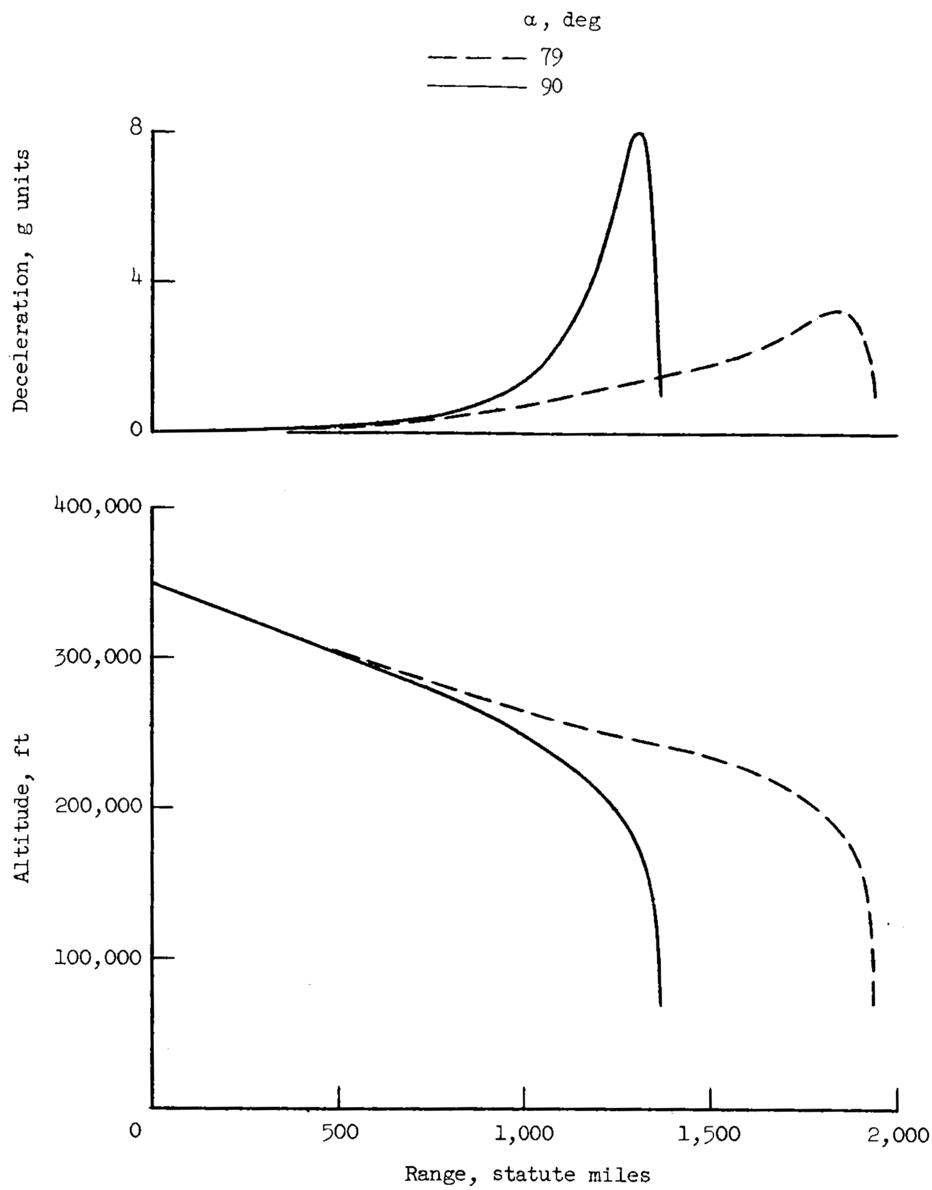

Figure 2.- Comparison of variation of range with altitude and deceleration for angles of attack of 90° and 79°. Nonrotating earth; V_o = 25,863 feet per second; γ_o = -1°; W/S = 20 pounds per square foot.

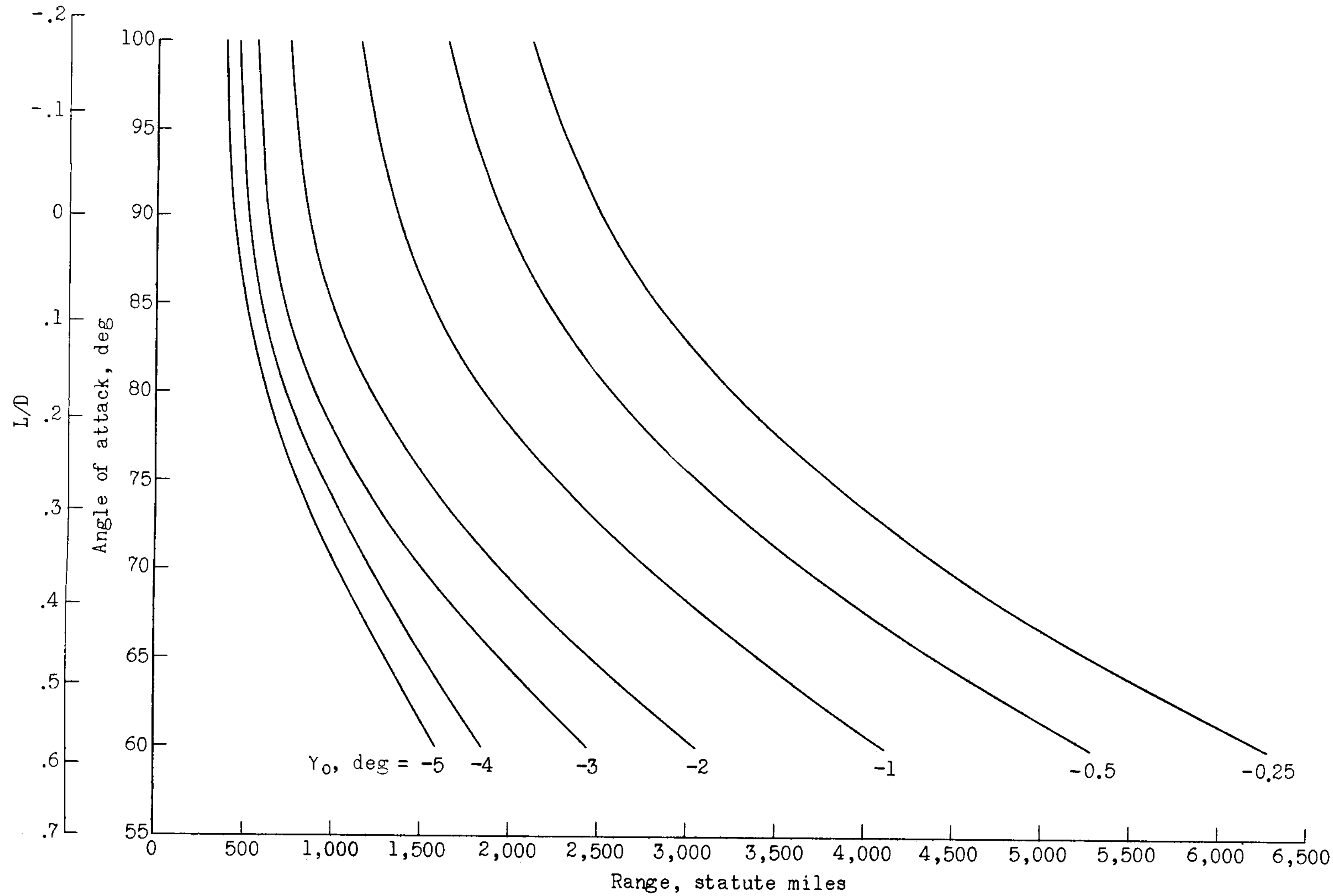

Figure 3.- Variation in range as a function of angle of attack and entry angle. Nonrotating earth; h_o = 350,000 feet; V_o = 25,863 feet per second; W/S = 20 pounds per square foot.

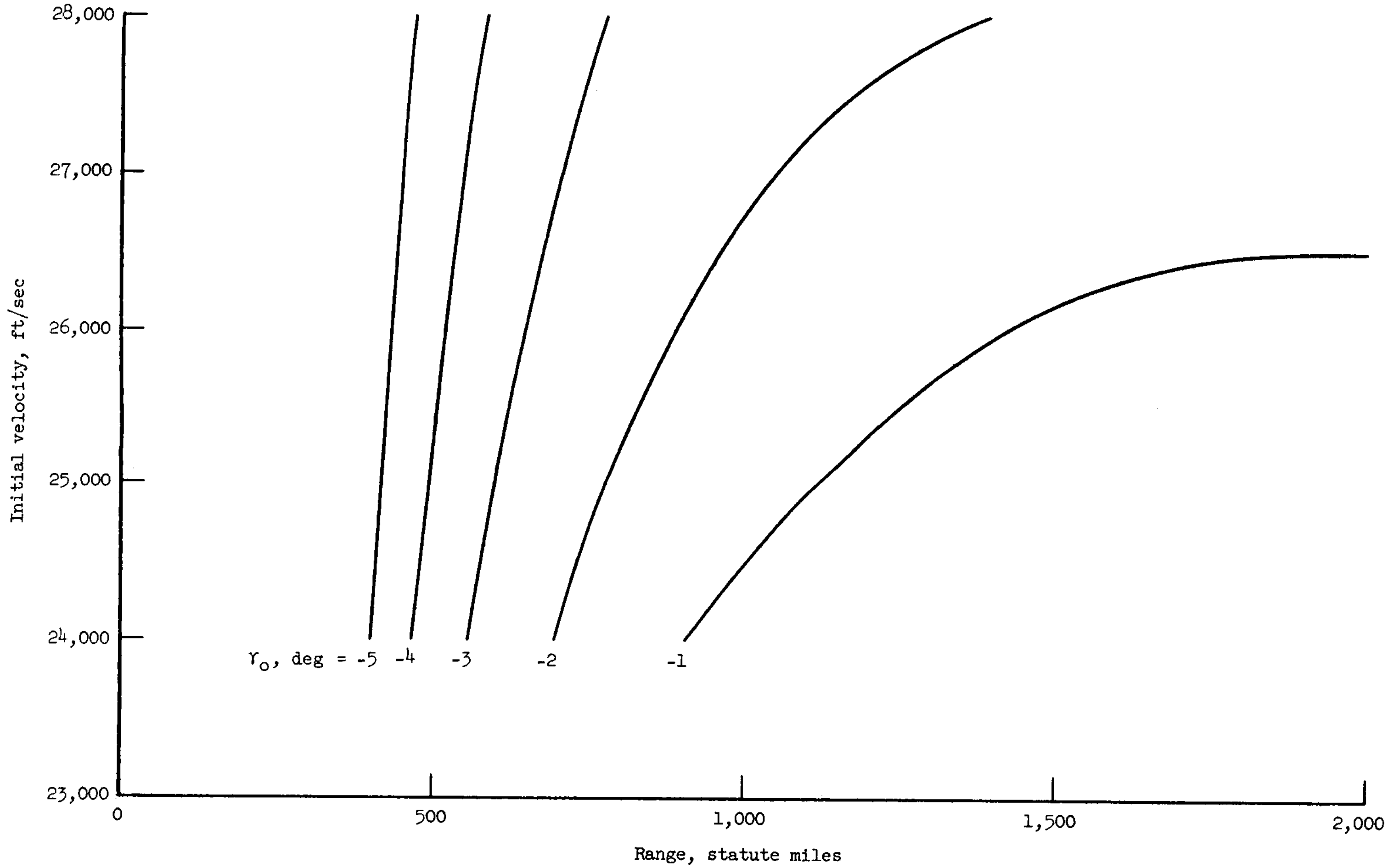

Figure 4.- Variation in range as a function of initial velocity and entry angle. Nonrotating earth; h_o = 350,000 feet; W/S = 20 pounds per square foot; $\alpha = 90^\circ$.

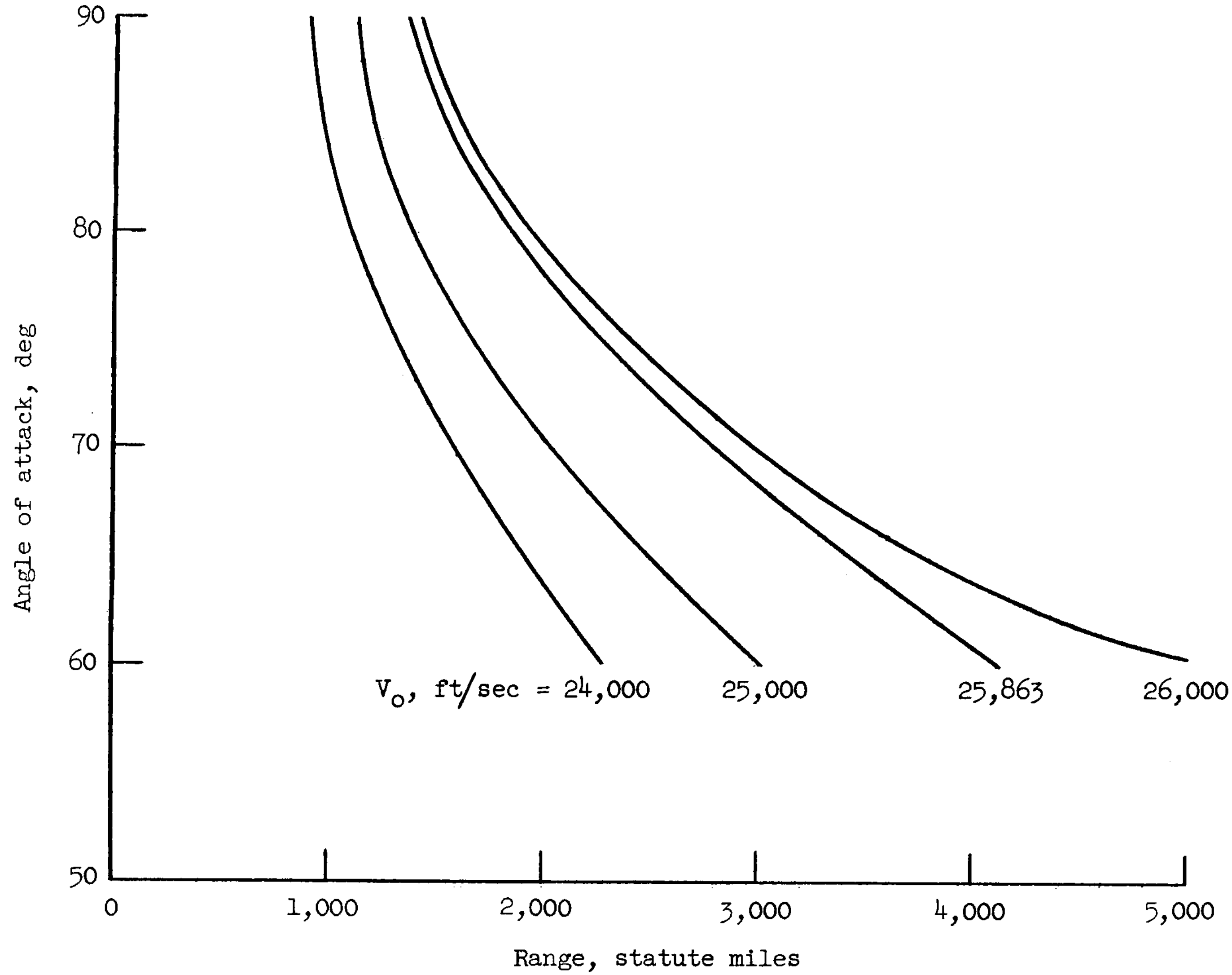

Figure 5.- Variation in range as a function of angle of attack and initial velocity. Nonrotating earth; h_o = 350,000 feet; $\gamma_o = -1^\circ$.

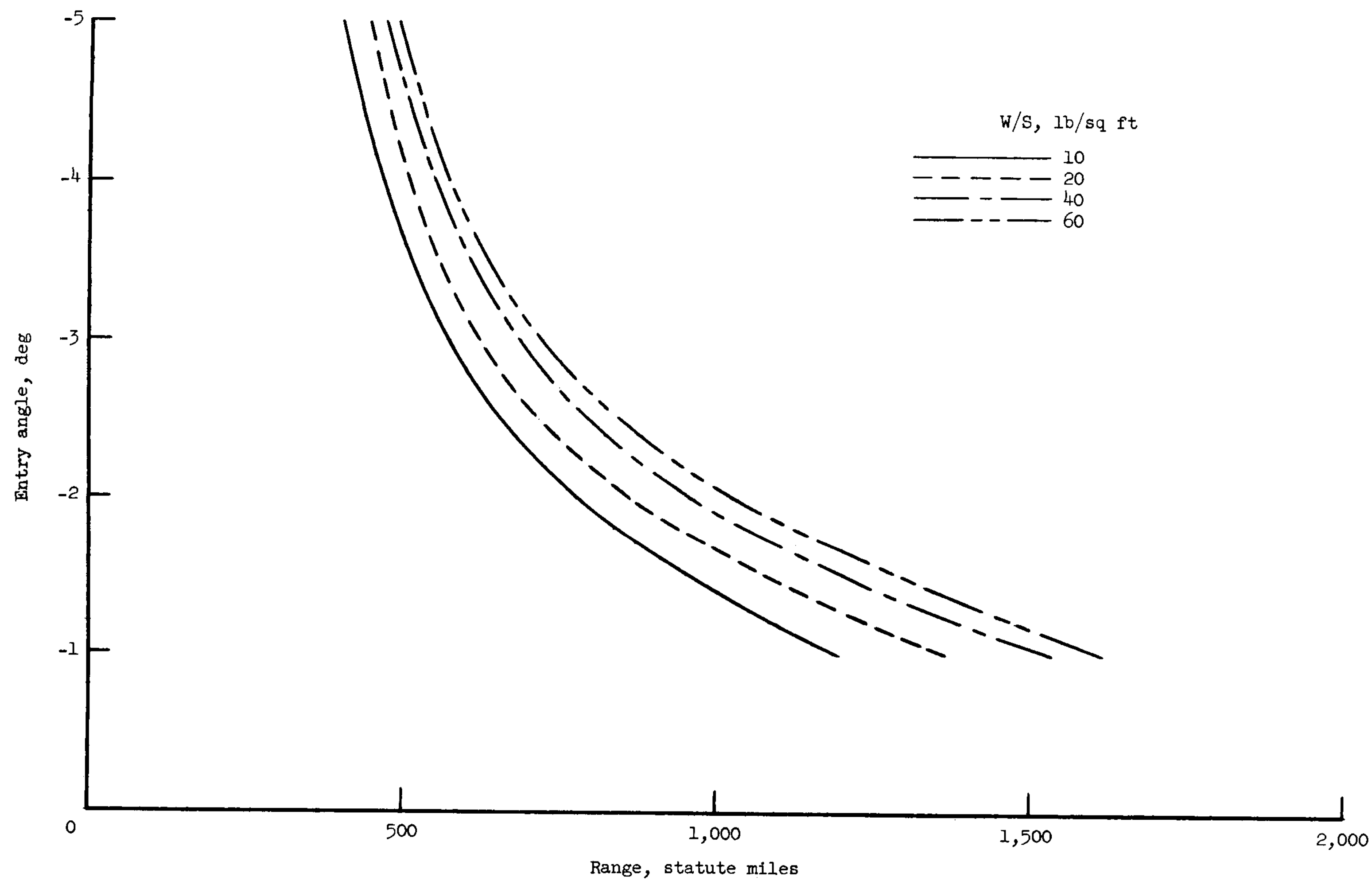

Figure 6.- Variation in range as a function of entry angle and wing loading. Nonrotating earth; $h_o = 350{,}000$ feet; $V_o = 25{,}863$ feet per second; $\alpha = 90^{\circ}$.

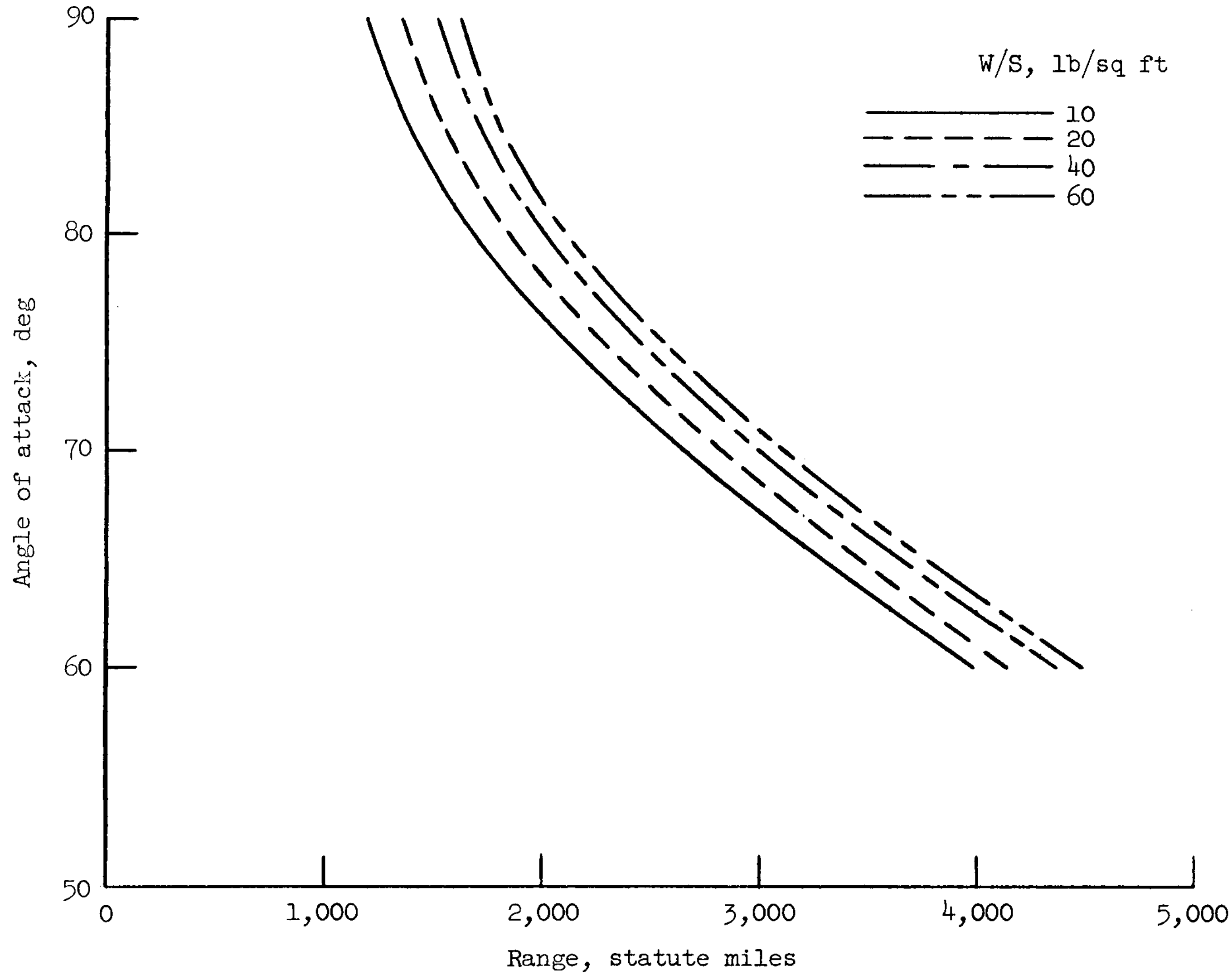

Figure 7.- Variation in range as a function of angle of attack and wing loading. Nonrotating earth; h_o = 350,000 feet; V_o = 25,863 feet per second; $\gamma_o = -1^o$.

L-830

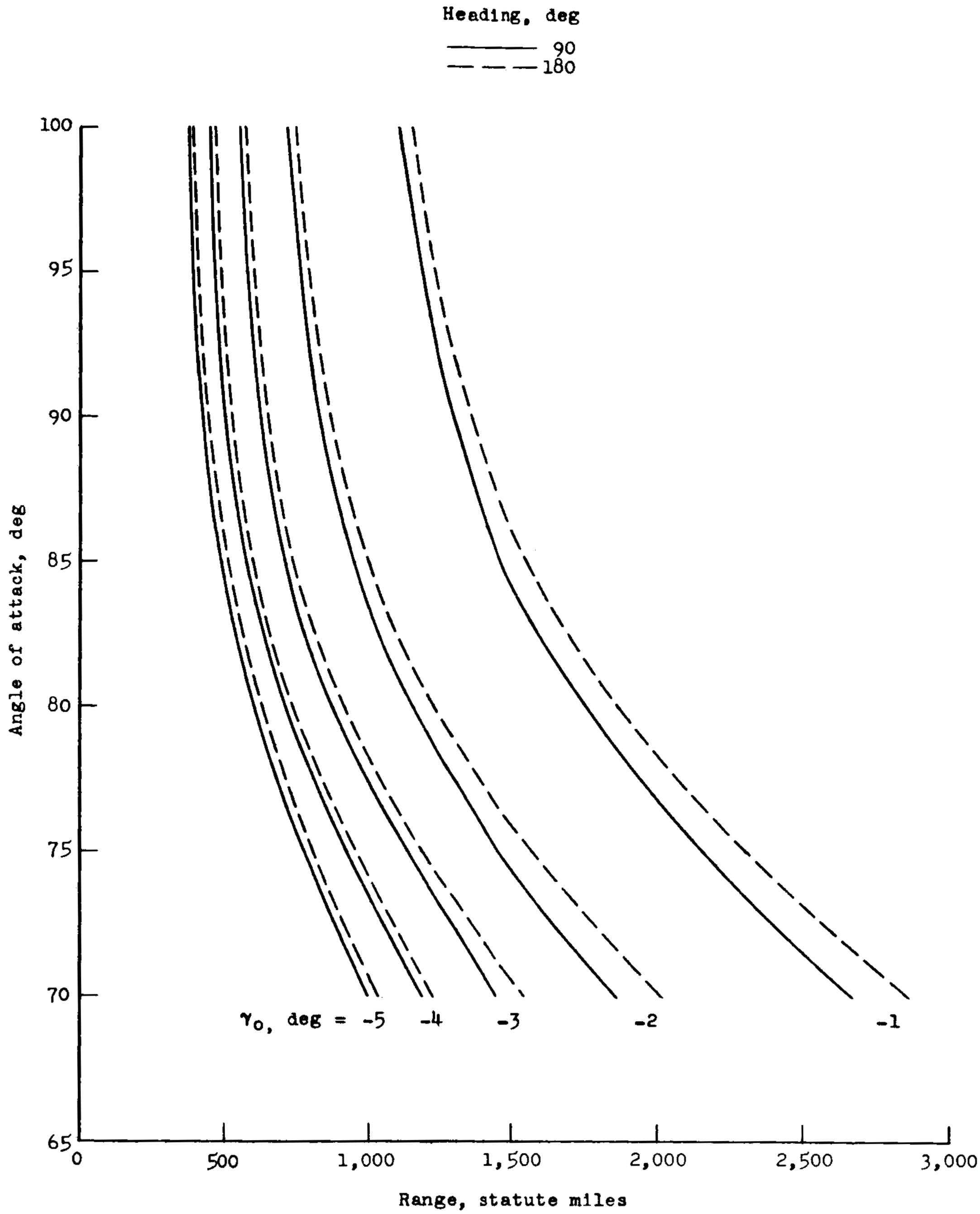

Figure 8.- Variation in range as a function of angle of attack and entry angle for headings of 90° and 180°. Rotating earth; h_o = 350,000 feet; V_o = 25,743 feet per second; W/S = 20 pounds per square foot.

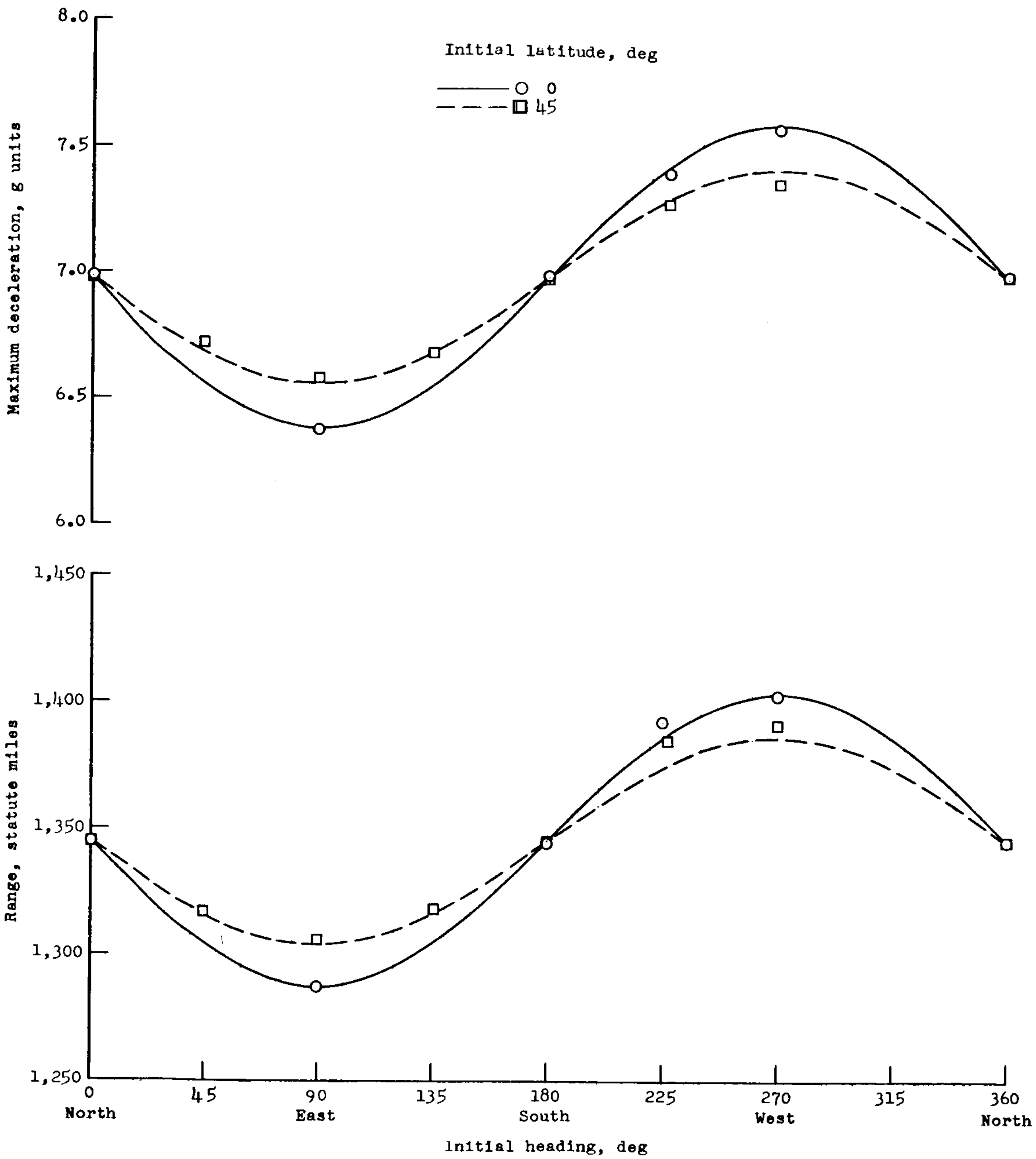

Figure 9.- Variation in range and maximum deceleration as a function of heading and initial latitude. Rotating earth; h_o = 350,000 feet; V_o = 25,743 feet per second; $\gamma_o = -1^o$; W/S = 20 pounds per square foot.

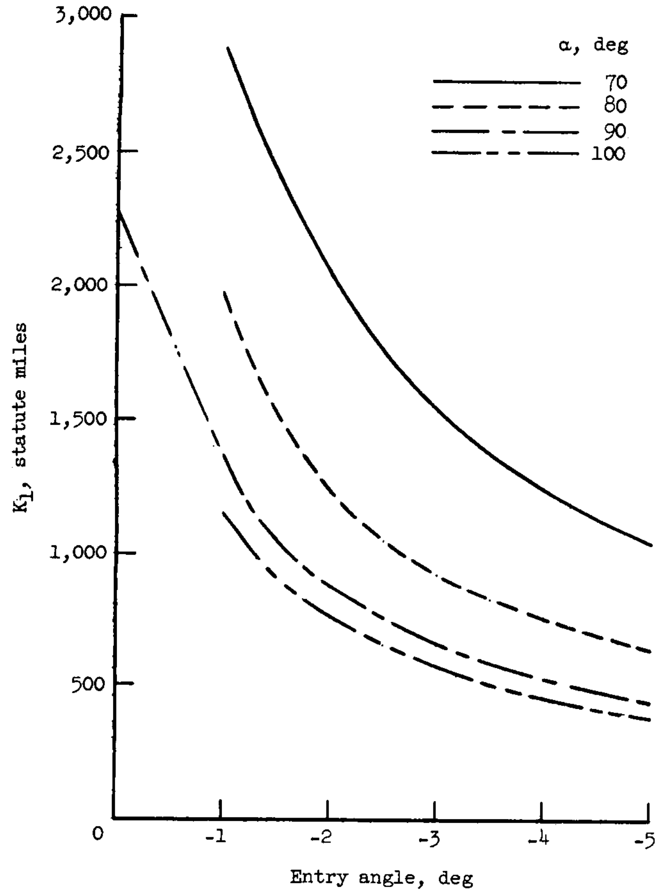

(a) Variation in K_1 as a function of entry angle and angle of attack.

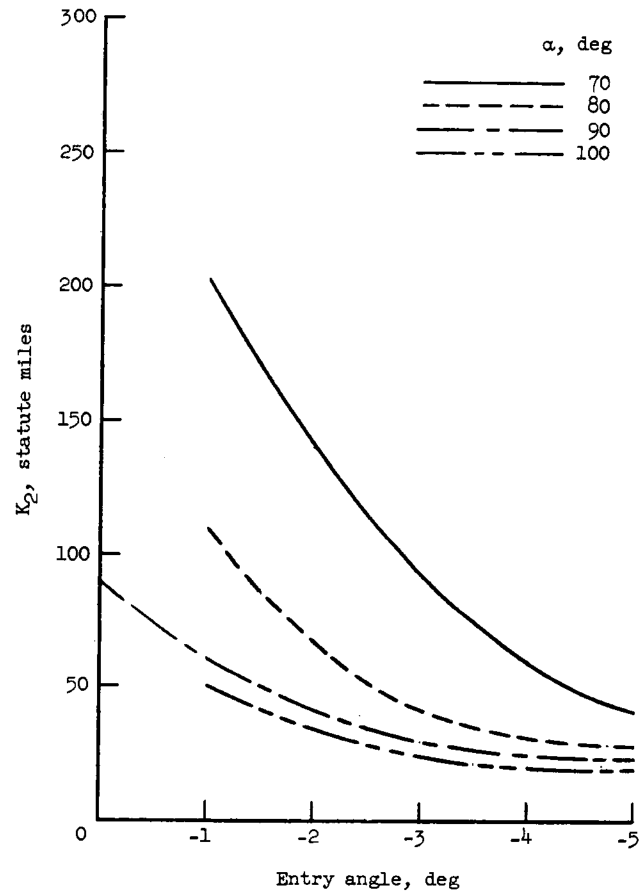

(b) Variation in K_2 as a function of entry angle and angle of attack.

Figure 10.- Variation in K_1 and K_2 as a function of entry angle of attack where range = $K_1 - K_2 \sin A \sin L$. Rotating earth; h_o = 350,000 feet; V_o = 25,743 feet per second; W/S = 20 pounds per square foot.

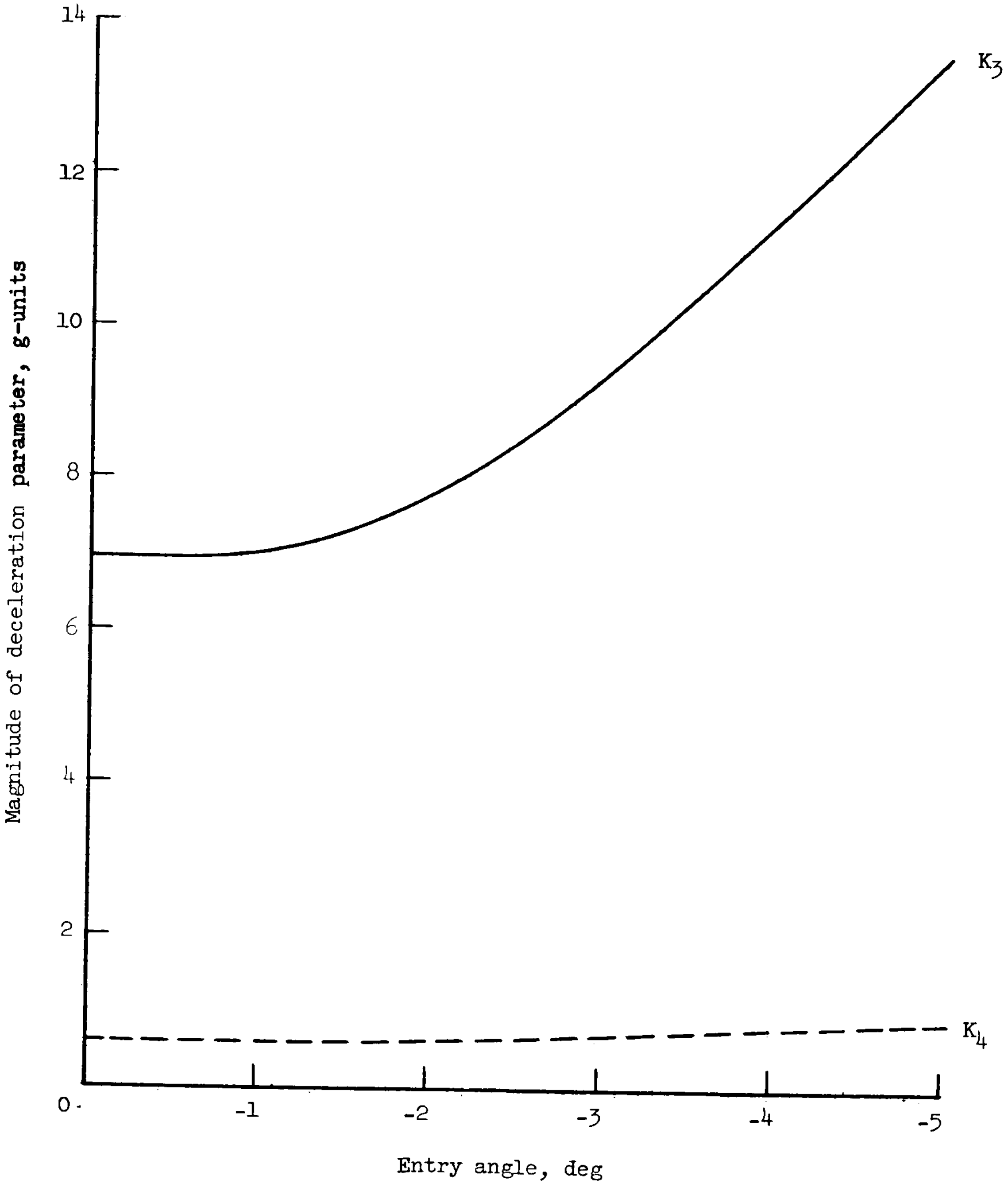

Figure 11.- Variation in K_3 and K_4 with entry angle where $g_{max} = K_3 - K_4 \sin A \sin L$. Rotating earth; h_o = 350,000 feet; V_o = 25,743 feet per second; $\alpha = 90^\circ$; W/S = 20 pounds per square foot.

L-830

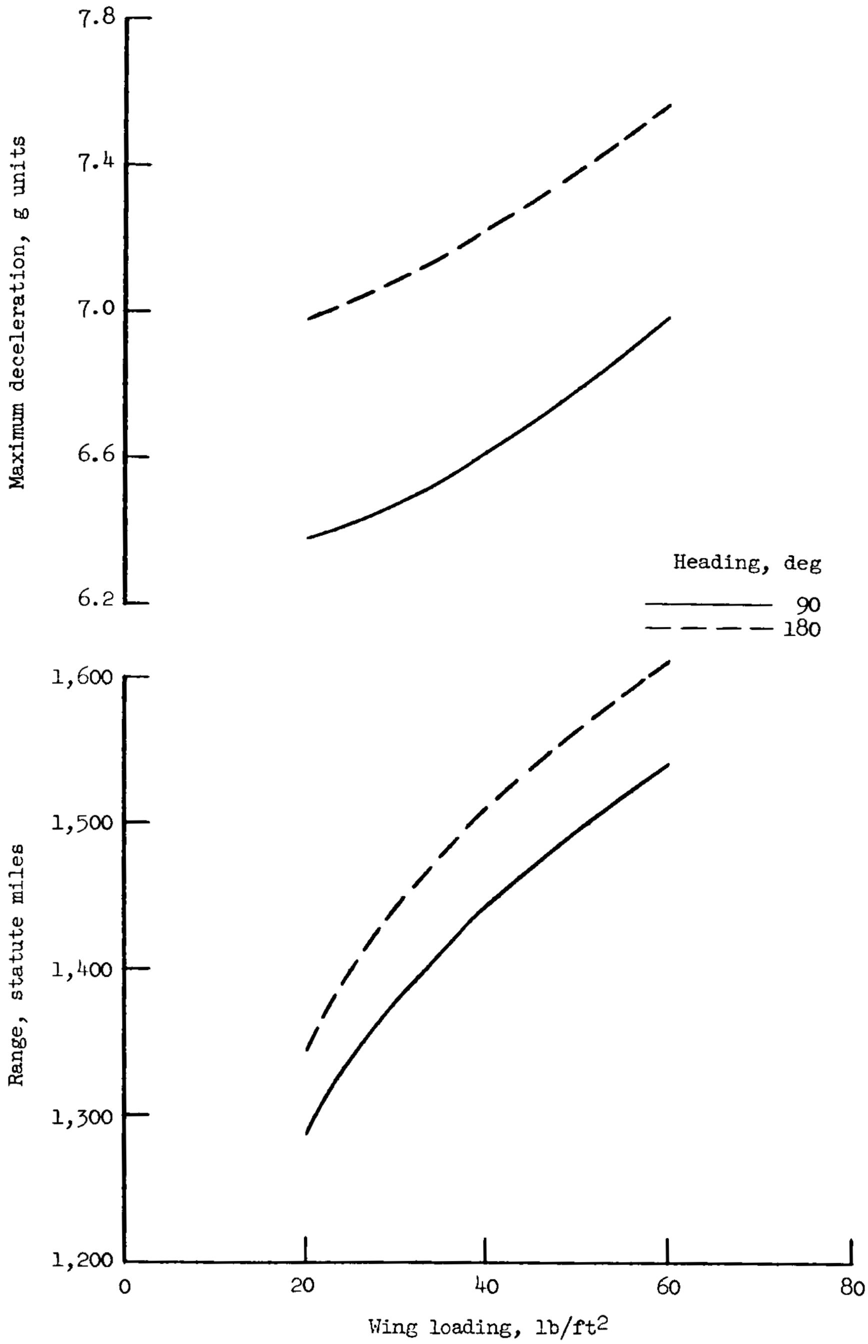

Figure 12.- Variation in range and maximum deceleration with wing loading for headings of 90° and 180°. Rotating earth; h_o = 350,000 feet; V_o = 25,743 feet per second; γ_o = -1°; α = 90°.

L-830

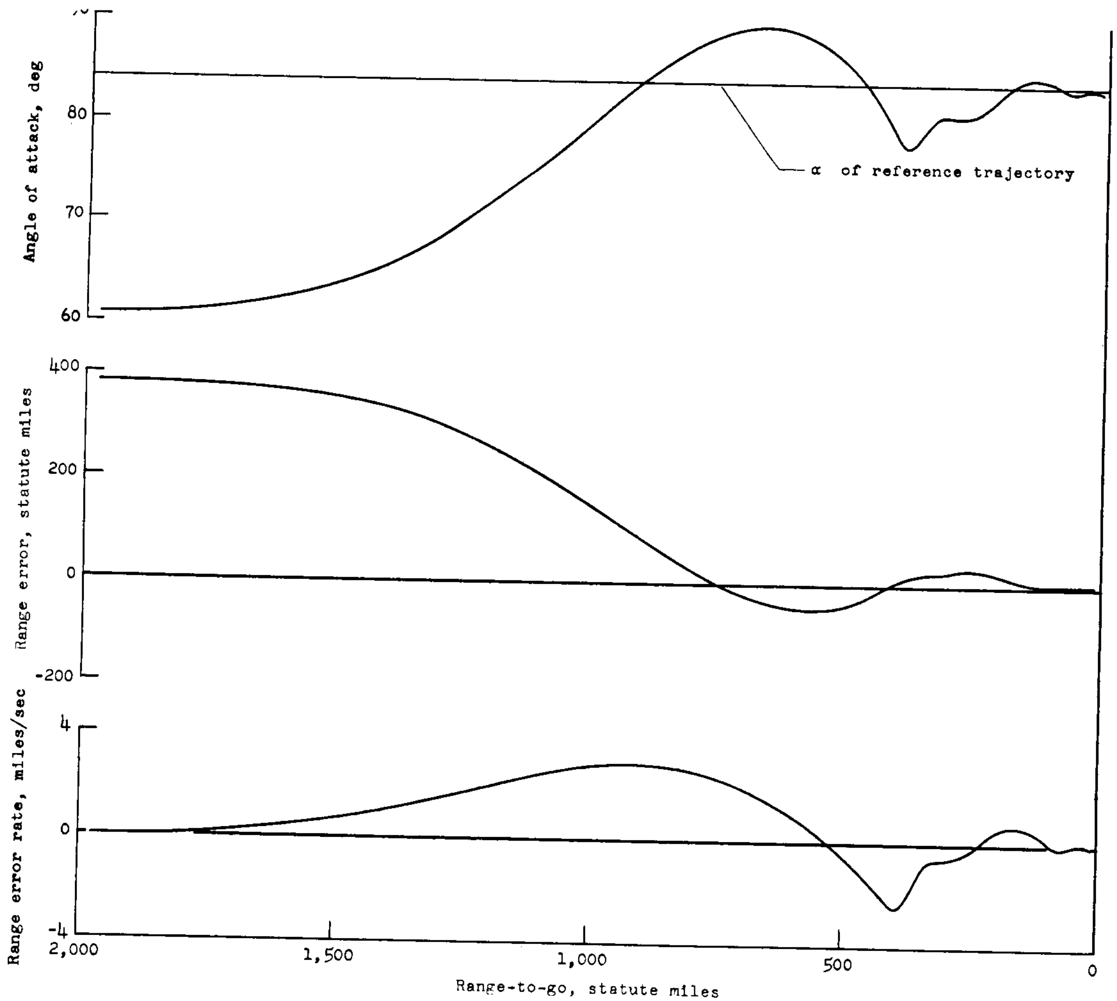

Figure 13.- Variation in angle of attack, range error, and range error rate with range-to-go for controlled trajectory. h_o = 350,000 feet; V_o = 25,863 feet per second; $\gamma_o = -1^o$; W/S = 20 pounds per square foot; $\alpha = 84^o - 0.06\epsilon_r - 2\dot{\epsilon}_r$.

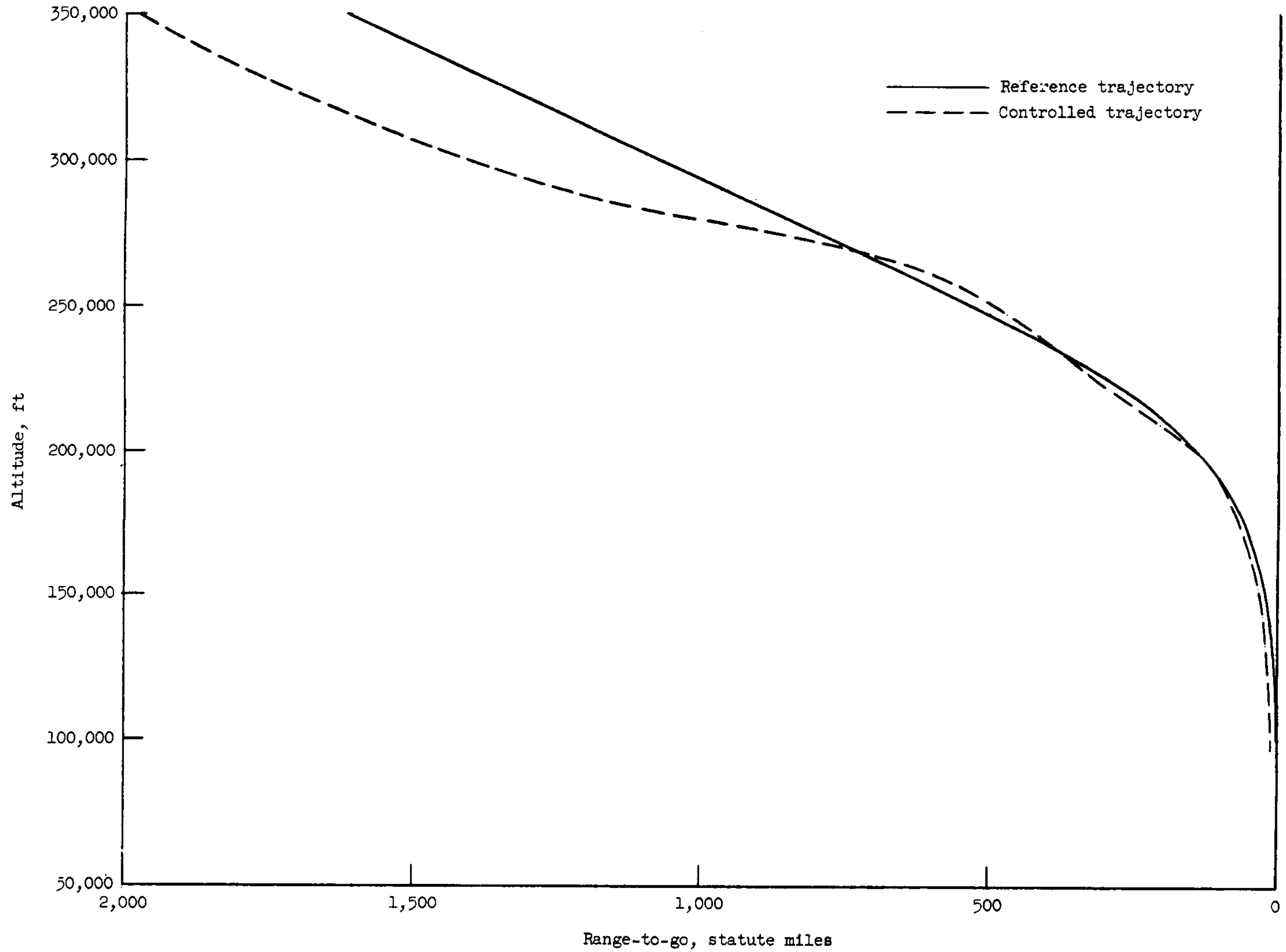

Figure 14.- Range-to-go as a function of altitude for reference trajectory and controlled trajectory. V_o = 25,863 feet per second; $\gamma_o = -1^\circ$; W/S = 20 pounds per square foot.

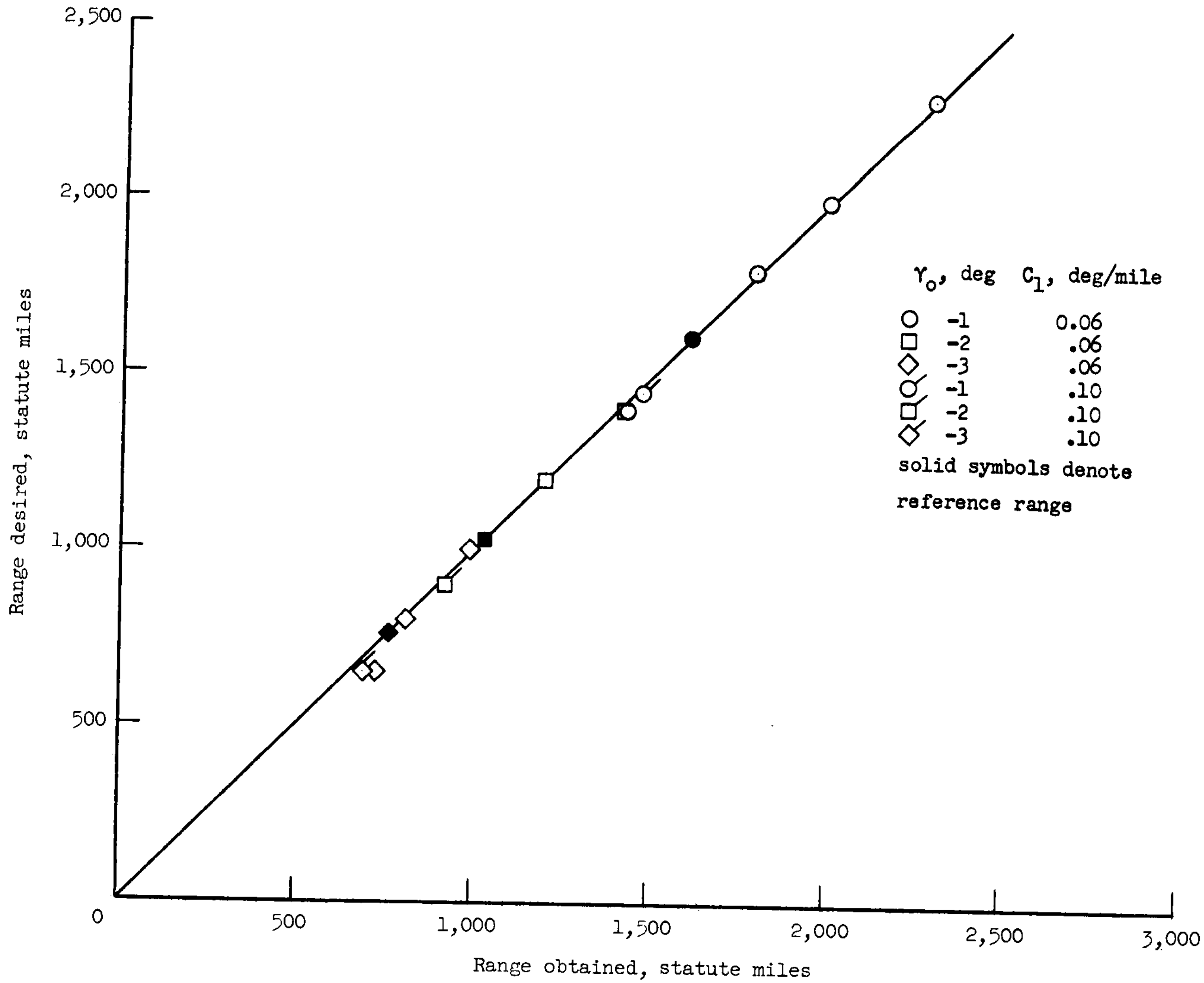

Figure 15.- Range obtained as a function of range desired for controlled trajectories. h_o = 350,000 feet; V_o = 25,863 feet per second; W/S = 20 pounds per square foot.

6J

L-830

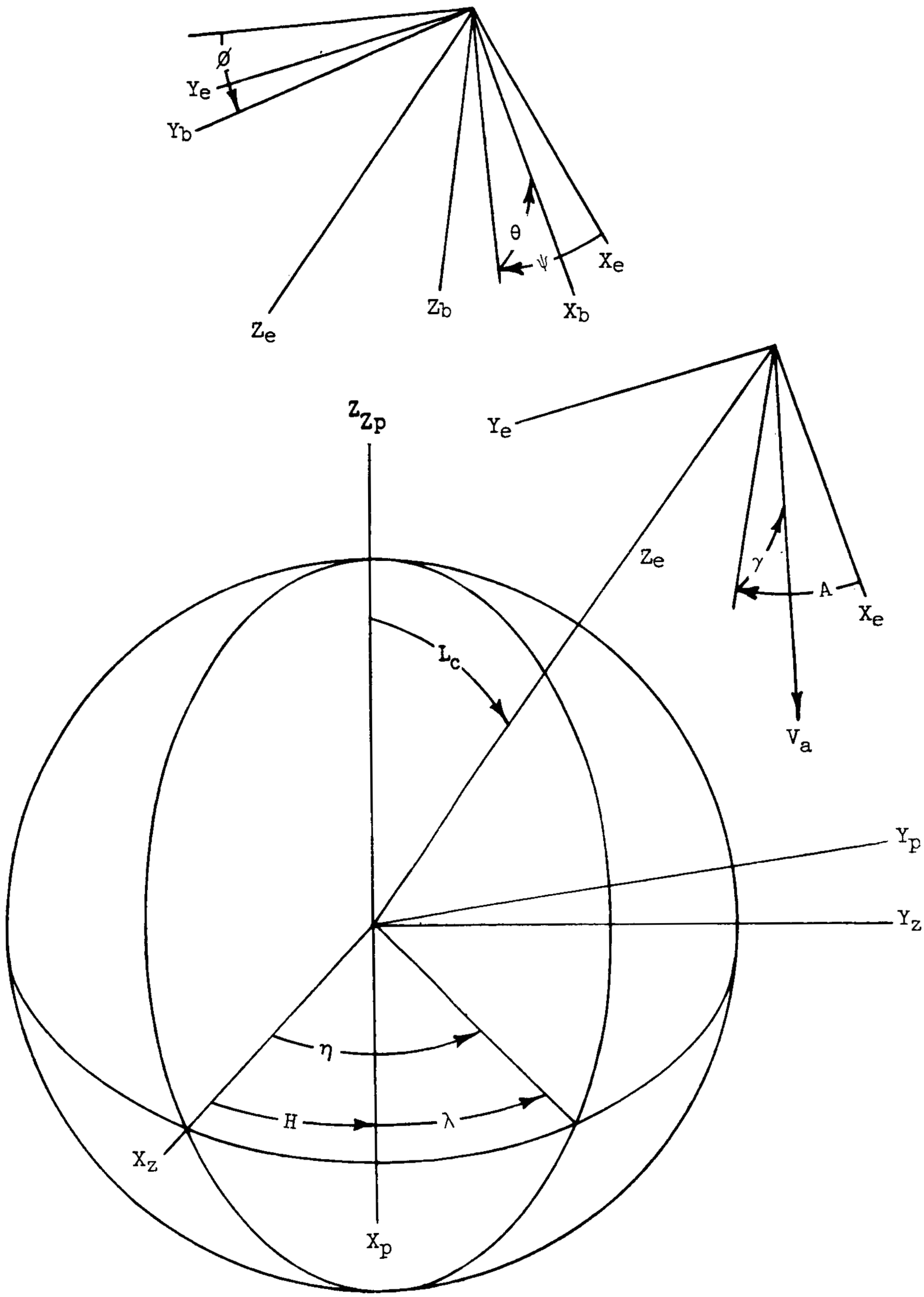

Figure 16.- Geometry of axes systems for rotating-earth analysis.